Taylor & Francis
Taylor & Francis Group

Corrosion Engineering, Science and Technology
The International Journal of Corrosion Processes and Corrosion Control

ISSN: 1478-422X (Print) 1743-2782 (Online) Journal homepage: http://www.tandfonline.com/loi/ycst20

Corrosion behaviour of Ni-based superalloys in molten FLiNaK salts

Niketan S. Patel, Viliam Pavlík, Blanka Kubíková, Martin Nosko, Vladimír Danielik & Miroslav Boča

To cite this article: Niketan S. Patel, Viliam Pavlík, Blanka Kubíková, Martin Nosko, Vladimír Danielik & Miroslav Boča (2018): Corrosion behaviour of Ni-based superalloys in molten FLiNaK salts, Corrosion Engineering, Science and Technology, DOI: 10.1080/1478422X.2018.1525829

To link to this article: https://doi.org/10.1080/1478422X.2018.1525829

CORROSION ENGINEERING, SCIENCE AND TECHNOLOGY
https://doi.org/10.1080/1478422X.2018.1525829

The Institute of Materials, Minerals and Mining

Taylor & Francis
Taylor & Francis Group

Corrosion behaviour of Ni-based superalloys in molten FLiNaK salts

Niketan S. Patel[a], Viliam Pavlík[a], Blanka Kubíková[a], Martin Nosko[b], Vladimír Danielik[c] and Miroslav Boča[a]

[a]Department of Molten Systems, Institute of Inorganic Chemistry, Slovak Academy of Sciences, Bratislava, Slovakia; [b]Institute of Materials and Machine Mechanics, Slovak Academy of Sciences, Bratislava, Slovakia; [c]Institute of Inorganic Chemistry, Technology and Materials, Slovak Technical University, Bratislava, Slovakia

ABSTRACT

High-temperature corrosion tests of alloys, Nimonic 80A, Inconel 718 and Inconel C-276, were investigated at 680°C in molten alkali fluoride salt (LiF–NaF–KF: 46.5–11.5–42%) environment. In this work, techniques included were weight loss measurements and potentiodynamic polarisation curves measurements. Inconel C-276 and Inconel 718 showed better corrosion resistance, while Nimonic 80A exhibited comparatively lower corrosion resistance. The high-temperature corrosion behaviour was observed using measurements of the oxide morphology and thickness. The corrosion rates were determined by recording the weight changes of the sample alloys at different time intervals. Microstructural examination showed the depletion of Cr near the surface of the alloys and hence the significant weight loss in the early stages of corrosion tests. The corrosion mechanism of the alloys is discussed in detail.

ARTICLE HISTORY
Received 11 May 2018
Revised 10 September 2018
Accepted 16 September 2018

KEYWORDS
High-temperature alloys; nuclear reactor materials; corrosion; oxidation; scanning electron microscopy SEM

Introduction

The use of molten salt technology as a working fluid has a proven success in many industrial applications. In fact, molten salts have been proposed for use in many energy conversion technologies mainly due to their potential as heat transfer agents and industrial liquid fuels. Molten fluoride salts possess several important properties: excellent thermal conductivity, stability at desired working temperatures, high boiling point, high specific heat and low viscosity [1]. Molten fluoride salts such as eutectic LiF–NaF–KF (FLiNaK) and LiF-BeF_2 (FLiBe) have been proposed for use as primary and secondary reactant coolants in molten salt reactors [2], advanced high-temperature reactor [3] and in solar power towers [4]. However, compatibility of molten fluoride salts with the structural alloys and materials corrosion has been of real concern at such temperatures (600–900°C). Hence, the material development and the corrosion studies turn out to be an essential part of the research. Materials derive corrosion resistance by formation of passive oxide film but in molten fluoride salt systems, passive oxide films are unstable and once the film is vanished, the least noble alloying element is selectively attacked by dissolution [1,5,6]. These three types of corrosion mechanisms are proposed for materials in static molten fluoride salts: intrinsic corrosion, corrosion by impurities, and galvanic corrosion [7]. Authors [2,8] presented a good selection of alloys studied in FLiNaK. It has been a constant rise in corrosion investigations reported in various molten salt environments from both theoretical and experimental viewpoints. However, corrosion studies of superalloys in molten fluoride salts are limited to only a handful of research teams globally and only few of them involved a varied range of alloys [2,8–11]. A more detailed and comprehensive literature review on high-temperature corrosion behaviour of superalloys in molten salts was recently published by [12], in an effort to give an in-depth insight of the recent developments that have occurred in the latter part of the last decade.

In this study, we investigated corrosion characteristics of alloys Nimonic 80A, Inconel 718 and Inconel C-276 in molten FLiNaK environments at temperature of 680°C. These experiments were carried out from 8 to 48 h of immersion period in an attempt to understand the corresponding corrosion behaviour of the tested alloys at given time intervals, respectively. In terms of superalloys corrosion, immersion period of 48 h signifies only the initial stages of corrosion but the previously reported studies proved that it's one of the most critical one [2,8,9]. Since a molten salt acts as an electrolyte, electrochemical techniques are also employed for 8 h immersion period. Various microstructural characterisation techniques were used to reveal the cross-sectional morphologies of the corroded samples and to evaluate corrosion attack depth.

Experimental

Materials and preparations

Three Ni-based alloys Nimonic 80A, Inconel 718 and Inconel C-276 (supplier Bibus Metals s.r.o, Czech Republic) were selected as the target materials for corrosion tests. The composition of the tested alloys is listed in Table 1. The samples were cut into 2 mm thick discs by a boron nitride blade (CBN-blade) on precision cutter Isomet 5000 (Buehler, U.S.A.). The samples were then prepared by mechanical polishing and grinding by Tegrapol 25 (Struers, U.S.A.) with a diamond suspension (1 μm). Then, the samples were ultrasonically cleaned in deionised water, dried in acetone and transferred to glove box in a desiccator. The exact dimensions of each sample were measured using a micrometre screw gauge (with a precision of 0.01 mm) and the weights before and after the experiment were recorded with highly precise

CONTACT Niketan S. Patel niketan.ptl@gmail.com Department of Molten systems, Institute of Inorganic Chemistry, Slovak Academy of Sciences, Dúbravská cesta 9, Bratislava 845 36, Slovakia

Table 1. Compositions of alloys.

Alloy/ composition (wt-%)	Ni	Cr	Fe	Co	Mo	W	Al	Mn	Ti	Si	Nb	Cu	O
Nimonic 80A	76.60	19.00	0.12	0.024	<0.01	<0.01	1.42	0.23	2.44	<0.01	<0.05	–	–
Inconel C-276	58.37	15.50	6.00	0.15	15.63	3.92	–	0.38	–	<0.01	–	–	–
Inconel 718	53.21	18.50	18.5	0.13	3.04	–	0.52	0.04	1.00	0.06	5.30	0.03	–

Table 2. Properties of FLiNaK.

Salt compounds/(mol-%)	46.5 LiF 11.5 NaF 42 KF
Melting point/(°C)	454
Boiling point/(°C)	1570
Heat capacity/(J g^{-1} K^{-1})	1.88
Thermal conductivity/(W m^{-1} K^{-1})	0.92
Density/(g cm^{-3})	2.02
Viscosity/(cP)	2.9

KERN analytical weighing balance (KERN ABT Merck, Germany).

FLiNaK salts were considered in this study because of its exceptional properties (Table 2). Eutectic FLiNaK salt was composed of LiF (Ubichem, UK, purity 99%), NaF (Merck, Germany, purity 99%), and KF (Fluka Chemicals, UK, purity 99.5%) at ratios of 46.5–11.5–42 mol-%, respectively. Salts were dried for 48 h in a vacuum drying chamber (JAVOZ, Czech Republic) at 130°C, then stored and mixed in a glove box (JACOMEX, provider Chromspec, Slovakia, Ar atmosphere, purity 99,9999%, MESSER, Slovakia, H_2O and O_2 < 1 ppm) before the corrosion experiments.

Immersion method

Weight loss for the Ni-alloy coupons was observed by the immersion method for 8, 24, 30 and 48 h period in molten FLiNaK. The coupons were prepared as described in the section above. The experimental setup for the corrosion test is given schematically in Scheme 1, Figure 1(a,b). The setup for the immersion tests is shown in Scheme 1, Figure 1(a). The crucibles (sintered Al_2O_3, 99%) were dried at 105°C before filling. For each individual experiment, 50 g of the mixture of FLiNaK was weighed, and homogenised in a glove box under an inert atmosphere and loaded into the crucible. Then, the crucibles with the coupons were immersed into the furnace and the reaction time was recorded after a temperature of 680°C was reached and resulted weight loss was measured and reported accurately. Weight loss measurements were performed and repeated three times to confirm the reproducibility of results.

Electrochemical method

Electrochemical techniques included potentiodynamic polarisation curves measurements. As shown in Scheme 1, Figure 1 (b), electrochemical cell consists of a three electrode system. Alloy coupons as working electrode, platinum crucible served as a counter electrode, platinum sheet ($S = 2$ cm^2) was used as a quasi-reference electrode. A platinum crucible containing 40 g of dried eutectic FLiNaK was placed in a closed laboratory furnace under an inert argon atmosphere (99.99%, Messer Tatragas) and traces of oxygen were removed on copper cuttings heated to 350°C. After melting, the molten mixture

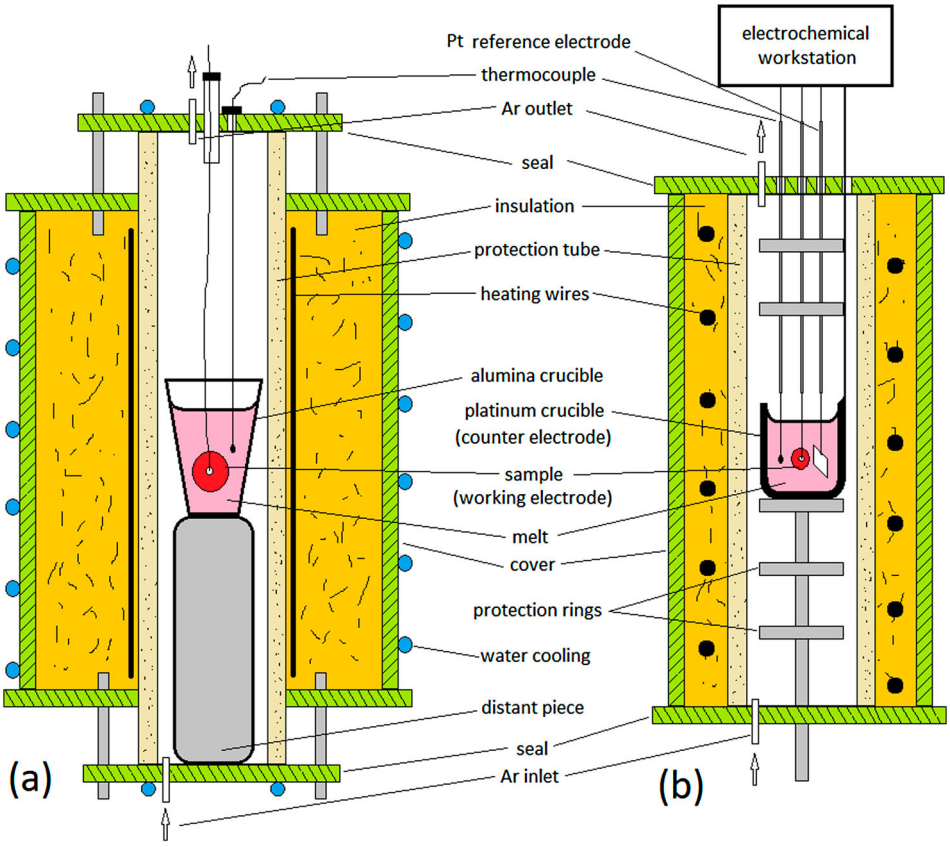

Figure 1. Schematic illustration of the experimental set up (a) corrosion rate measurements by immersion method (b) corrosion rate measurement by electrochemical method.

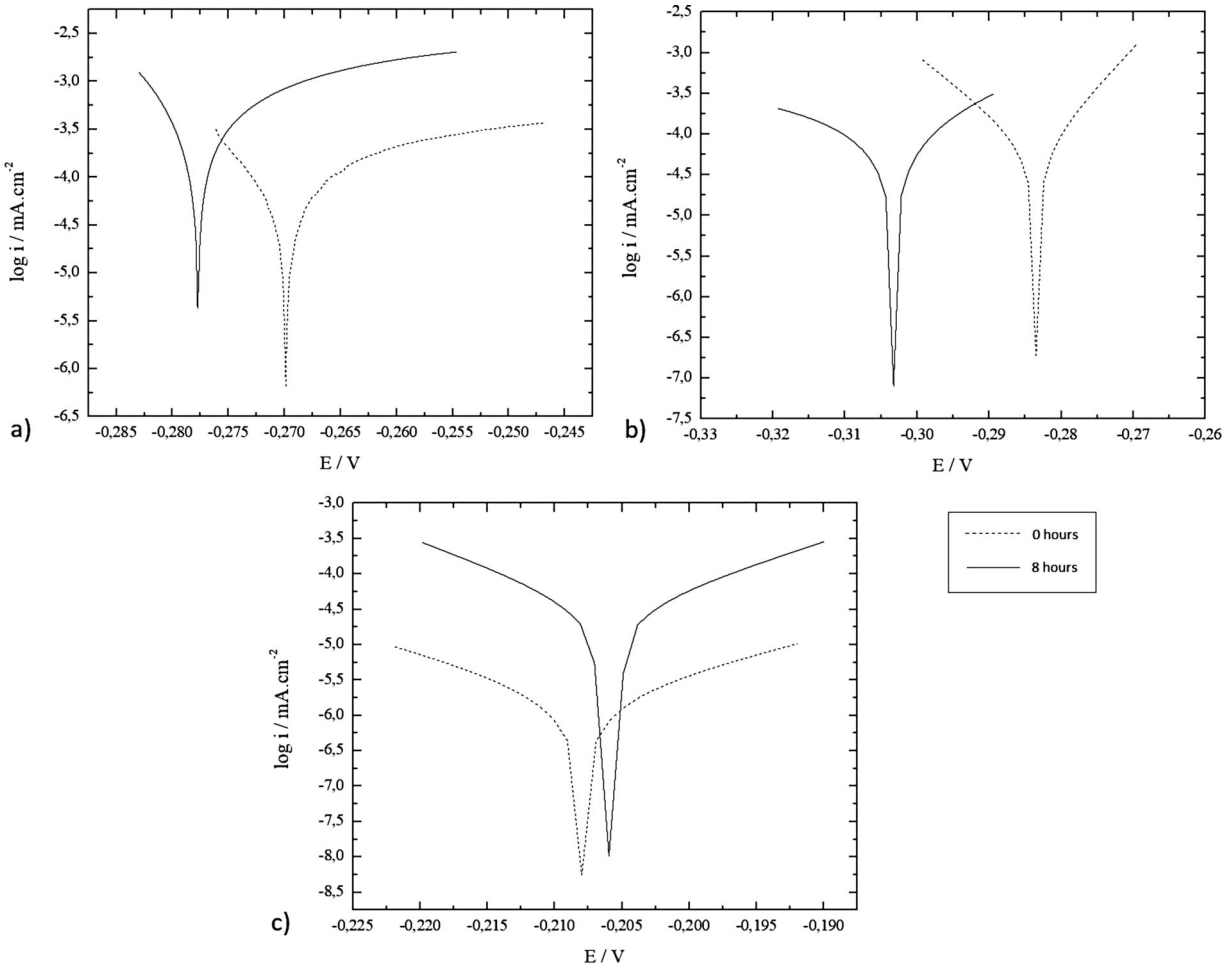

Figure 2. Potentiodynamic polarisation curves of (a) Nimonic 80A (b) Inconel 718 and (c) Inconel C-276 at 680 °C in contact of molten FLiNaK (0 hrs mentioned as initial and 8 hrs as final measurements).

was kept at a constant temperature of (680 ± 2)°C, controlled by a Pt–Pt10Rh thermocouple. After an immersion of alloy sample, the sample was kept at hold for 15 min in the melt before the starting of the electrochemical measurements. This time is necessary to achieve a quasi-stationary state after the initial immersion. The electrochemical measurement has been repeated after 8 h of the contact of the metal with the melt. Electrochemical measurements were performed using Solartron SI 1260A (Solartron Analytical, U.S.A.).

Microstructural characterisation

Scanning electron microscopy (SEM) (JEOL7600F, Japan, Co lamp) in combination with electron dispersive spectroscopy (EDS) (Oxford Instruments Ltd., UK) was used for the superficial and cross-sectional microstructure observation. Electron gun voltage was set to 15 kV to assure sufficient extraction energy and to quantify chemical composition; Co standard was used before measurement. The samples for microstructural observation were prepared via standard metallographic methods such as grinding and polishing. No additional etching was used.

Table 3. Corrosion potentials and corrosion current densities determined by Tafel linear fitting of polarisation curves for the tested alloys in FLiNaK at 680°C.

	Initial measurements	Final measurements (8 h contact with the melt)		
Alloy	E_{corr}/(V)	I_{corr}/(mA cm^{-2})	E_{corr}/(V)	I_{corr}/(mA cm^{-2})
Nimonic 80A	−0.270	0.1896	−0.278	0.6599
Inconel 718	−0.284	0.0522	−0.303	0.1401
C-276	−0.208	0.0017	−0.206	0.0029

Results and discussion

Potentiodynamic polarisation measurements

Figure 2 shows the potentiodynamic polarisation curves of Nimonic 80A, Inconel 718 and Inconel C-276 in molten FLiNaK at 680°C for initial and final (8 h), respectively.

In Table 3, corrosion potential (E_{corr}) and the corrosion current density (I_{corr}) calculated using Tafel extrapolation method are listed.

The corrosion potential of the Inconel C-276 versus platinum electrode was registered to the value of −208 mV, whereas Inconel 718 and Nimonic 80A showed relatively negative E_{corr} values. After 8 h of contact with molten FLiNaK, the obtained corrosion current densities were higher when compared with the initial stage. I_{corr} values for Inconel C-276 was lowest at 0.0029 mA cm^{-2} while Nimonic 80A showed relatively higher I_{corr} at around 0.66 mA cm^{-2}.

Immersion method

Nimonic 80A, Inconel C-276 and Inconel 718 alloys have been acquired and tested in the molten FLiNaK salt mixture

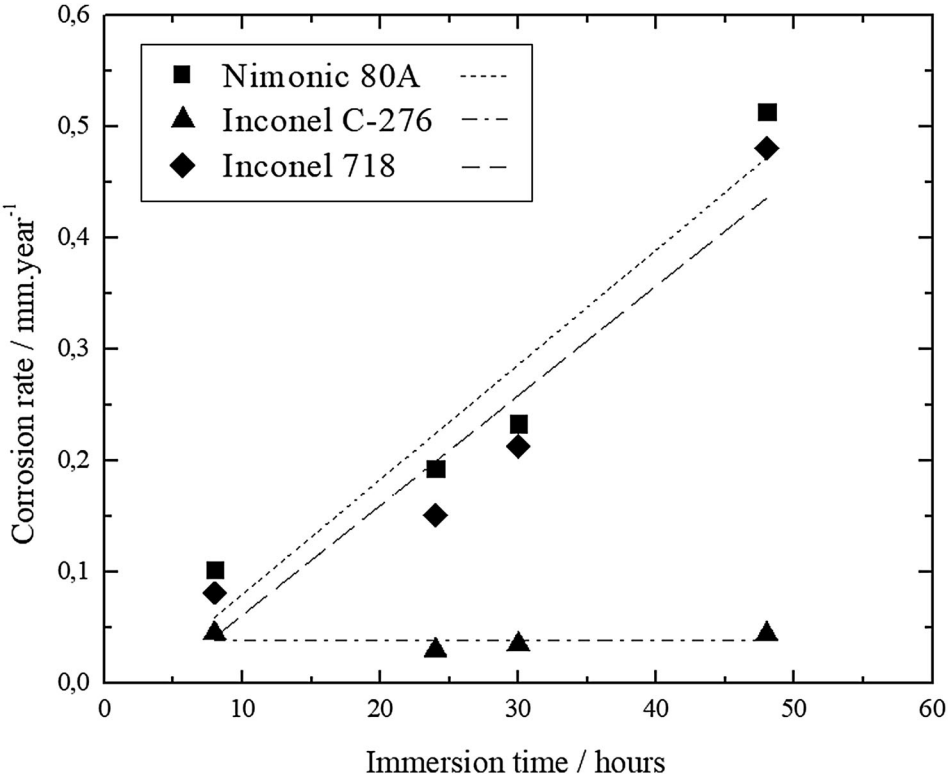

Figure 3. Plot of corrosion rates of the tested alloys in molten FLiNaK at 680°C versus immersion durations.

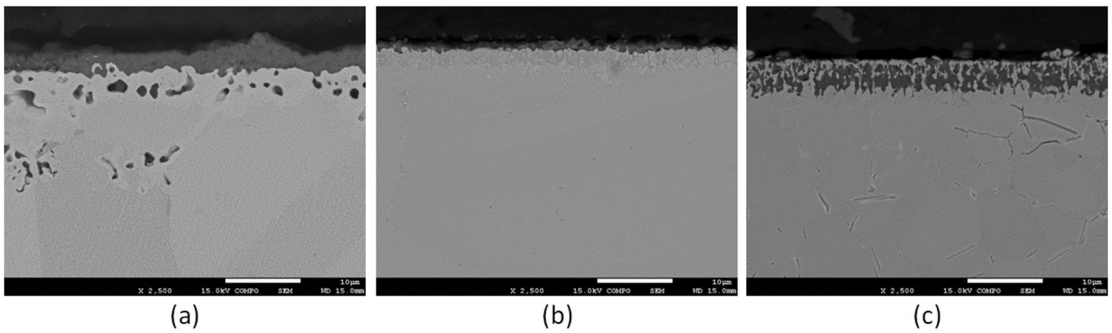

Figure 4. Cross-sectional SEM images of the microstructure of the corrosion layer of studied alloys in molten FLiNaK after 24 h of immersion period; Nimonic 80A (a), Inconel C-276 (b) and Inconel 718 (c).

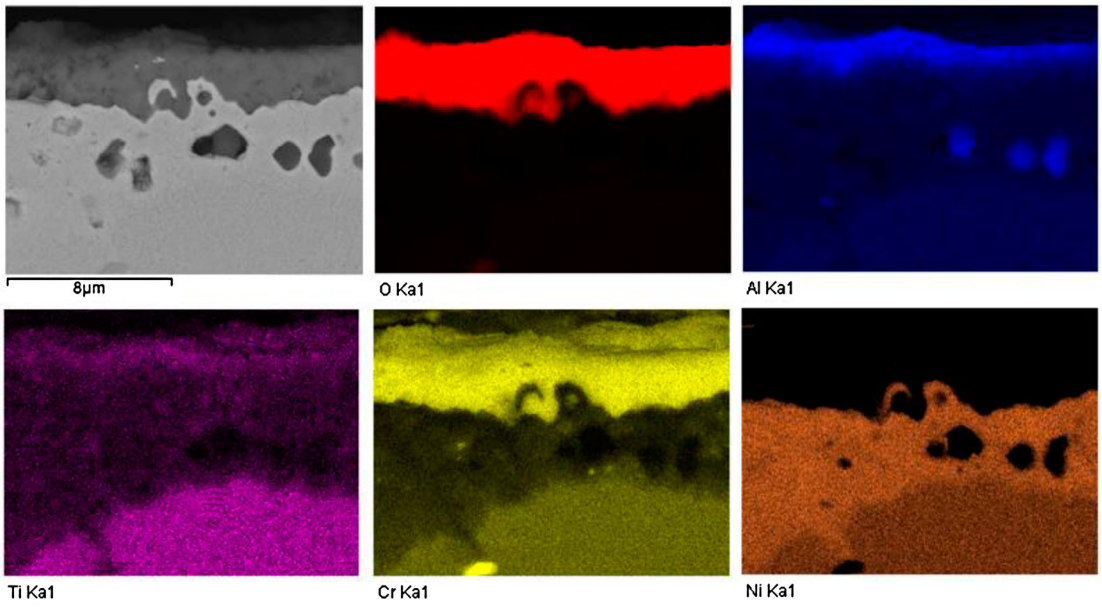

Figure 5. Cross-sectional microstructures and EDS elemental mapping of corrosion layer of Nimonic 80A in molten FLiNaK after 24 h of immersion period.

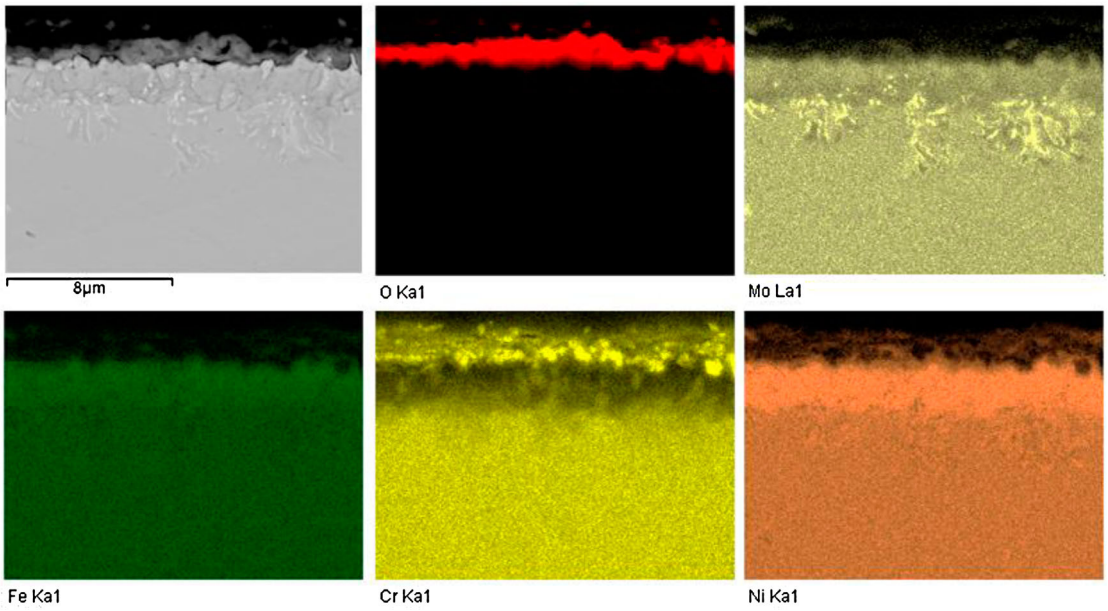

Figure 6. Cross-sectional microstructures and EDS elemental mapping of corrosion layer of Inconel C-276 in molten FLiNaK after 24 h of immersion period.

at 680°C for the immersion period of 8, 24, 30 and 48 h, respectively. Figure 3 shows corrosion rates of the tested alloys in terms of exposure duration.

The corrosion rates were calculated from the values of the weight loss before and after the immersion tests. The results of the weight change measurements showed that the weight loss increased with the Cr content of the alloys as Cr acts as one of the most reactive constituent. However, Inconel C-276 and Inconel 718 with similar Cr levels, but that Fe in Inconel 718 is mostly replaced by Mo in Inconel C-276 and Inconel C-276 showed much better corrosion resistance, suggests that Mo is resistant to corrosion in molten FLiNaK salt [2]. Although, the roles this alloying elements such as Mo, Fe, Co and W plays in corrosion resistance in molten fluoride salts is very complex and to study that weight loss results are supported with cross-sectional SEM and EDS elemental analysis.

Figure 4 shows the cross-sectional morphologies of the tested alloys in molten FLiNaK for immersion of 24 h for comparisons. The observed oxidation of materials near the surface after corrosion tests varies considerably for the tested alloys. Although, no significant intergranular attack was witnessed for any of the alloys examined for up to 24 h immersion period. In the first 24 h of each experiment mainly oxidation takes place and initial Cr-oxides were formed near the entire surface. From a thermodynamic point of view, Cr_2O_3 is the most stable oxide in the case of Ni–Cr–Fe-based alloys [13].

Figures 5–7 shows the cross-sectional microstructure and EDS elemental mapping of the tested alloys after 24 h immersion testing at 680°C in molten FLiNaK. The images show that clear oxide layers were formed at the surface of all the examined alloys. However, the width of the oxide layer varies in size; it is approximately 4 μm in case of Nimonic 80A, less than 2 μm for Inconel C-276 and about 8 μm for Inconel 718. Thus, just by comparing the depth of corrosion attack, Inconel C-276 showed better performance. This also confirms that the depth of corrosion attack is

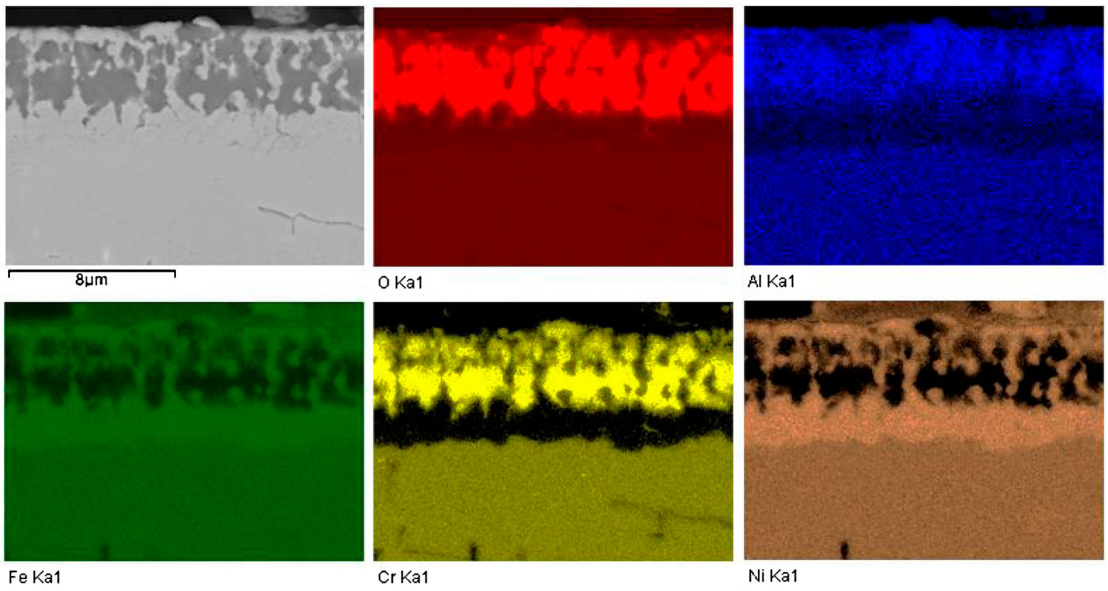

Figure 7. Cross-sectional microstructures and EDS elemental mapping of corrosion layer of Inconel 718 in molten FLiNaK after 24 h of immersion period.

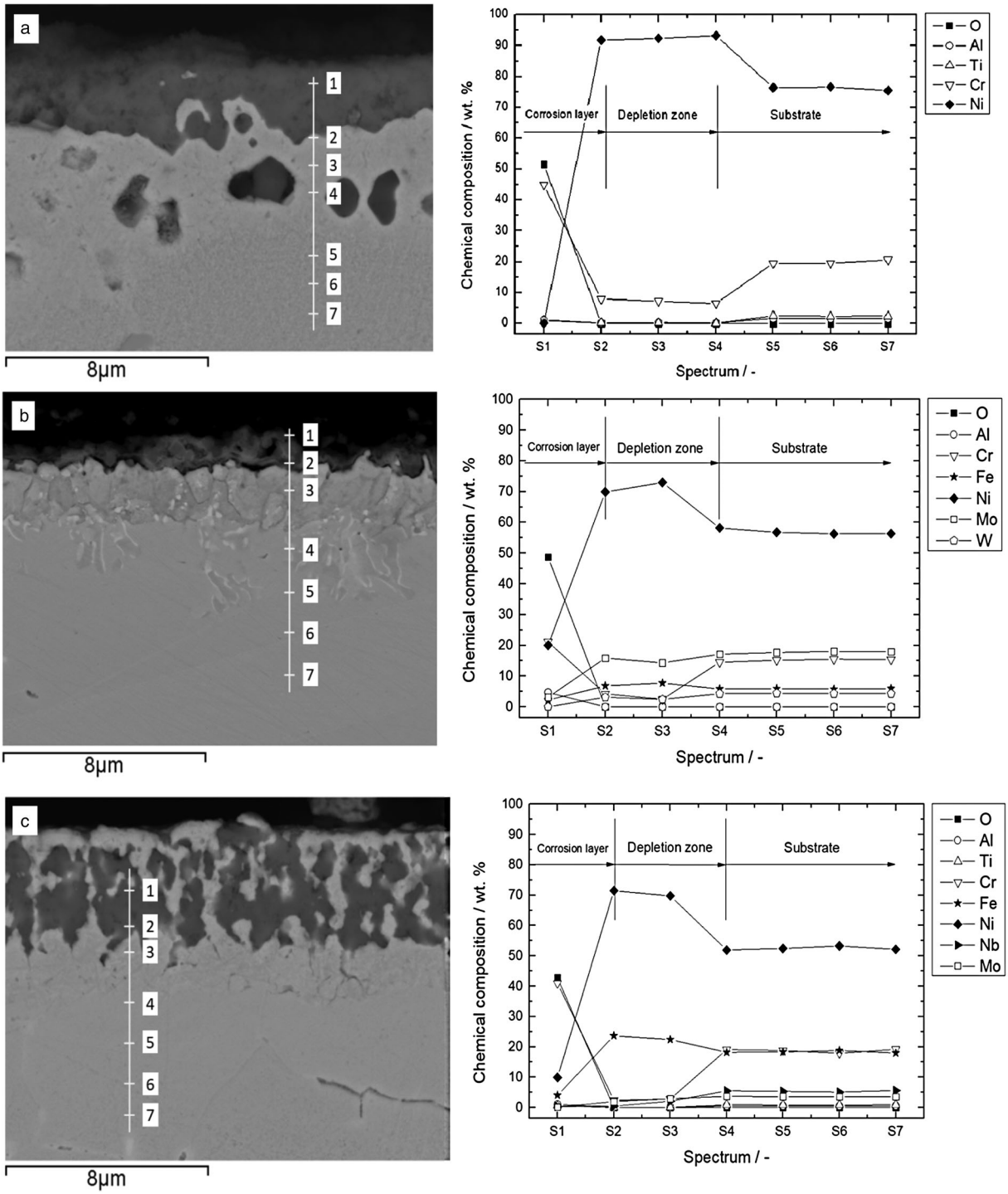

Figure 8. SEM cross-sectional image (left) with EDS elemental line scan (right) through corrosion layer and base metal and chemical quantitative analysis of the spots (a) Nimonic 80A (b) Inconel C-276 and (c) Inconel 718

proportional to weight loss [14]. But in our case, it is valid only for Nimonic 80A and Inconel C-276. This may be due to the study of initial stage corrosion only. In the case of long-term corrosion, the above-mentioned statement holds true in most occasions.

With the increase of time from 8 to 48 h, Cr in the matrix is depleted to form corrosion layer and beneath these oxide layers, distinct Cr depleted zones were observed for the tested specimens as can be seen in Figure 5–7. Molten salt analysed by XRD after the 24 h immersion period was free from corrosion precipitates suggest that corrosion products formed on the surface remained intact. Oxygen impurity in the experiments may occur due to the alumina crucible used, although appropriate steps were followed to avoid this problem.

Nimonic 80A showed dense and continuous corrosion layer. Figure 5 shows a defined accumulation of Cr in the corrosion product layer; Al is also present in the same zone with O as well. Ti is also oxidised just beneath the corrosion layer. Based on that, Cr_2O_3 and Al_2O_3 are suggested to exist in the outer corrosion layer.

Inconel C-276 exhibited thin but continuous and adherent corrosion layer. Figure 6 also showed a distinct build-up of Cr in the corrosion layer, however, Fe is not present in the product layer. The zone of higher concentration of O matched that of Cr. Mo is absent from that zone but concentrated phases of Mo was observed beneath the depletion zone. This may indicate the role of Mo in enhancing the corrosion resistance on Inconel C-276 alloy.

Corrosion layer formed for Inconel 718 in molten FLiNaK was significantly different from Nimonic 80A and Inconel C-276. As shown in Fig. 7, Cr oxide phase is beneath the intermetallic compound layer. This is due to the diffusion of oxygen into the alloy matrix, forming an oxygen reach area and then the alloying elements diffused out of the corrosion layer [13].

Figure 8 shows the cross-sectional microstructures and EDS elemental line scans of Nimonic 80A, Inconel C-276 and Inconel 718 after 24 h immersion testing at 680°C in molten FLiNaK. Chemical composition of the elements plotted against particular spots provides clear insight of the formation of the oxide layers and dissolution of susceptible elements into the molten salt environment. Spot S1 in all the alloys is positioned in a distinct dense oxide layer formed at the surface of the specimen. Spots S2 to S4 are located underneath the oxide layer and rest of the spots represents the base metal composition.

In case of Nimonic 80A and Inconel 718, Cr is more than 40% at S1, although, Inconel C-276 showed only slight increase in Cr levels. This relatively high content of Cr in the outer corrosion layer confirms the formation of Cr_2O_3 in the early stage of corrosion. This favourable Cr dissolution creates a Cr-depleted zone along the substrate beneath the oxide layer. As can be noticed in Figure 8, there is formation of a Ni-rich zone right underneath the oxide layer. This accumulated Ni inhibits the further diffusion of oxygen because it has weaker oxygen affinity than Cr [15]. Thus, the formation of Ni-rich zone beneath the oxide layers or in an inner corrosion layer may prevent internal oxidation and corrosion [16].

The results obtained from electrochemical tests and weight loss measurements indicated that Inconel C-276 outperformed in terms of corrosion rates. Inconel C-276 (16% Cr) also showed Cr dissolution, as Cr was expected to be selectively attacked due to the very negative Gibb's free energy of its fluoride phase. However, with highest Mo content (16%) Inconel C-276 showed Mo-rich precipitates beneath the depletion zone, confirming that Mo is usually resistant to corrosion in molten FLiNaK [2]. In contrary, Mo is replaced by Fe in Inconel 718 which showed higher corrosion rates. Moreover, Inconel 718 showed Cr oxide phase beneath the intermetallic compound layer.

Nimonic 80A has higher Ni content (76%) compared to the other two alloys. It can be assumed that higher the nickel content, lower is the corrosion rate. However, pure Ni is poorly resistant to corrosion in molten salts [17,18]. Nimonic 80A mainly contains Ni and Cr, and with large potential difference between Ni and Cr [19], the corrosion resistance of this alloy may suffer considerably. Another reason could be the absence of alloying elements such as Mo, Fe, Co and W, which plays an important role in general corrosion resistance in molten fluoride salts. Nimonic 80A showed higher corrosion rates and we could assume that has occurred due to the above-mentioned reasons. These results attained in this paper provide significant base and rich promise for the future trends of investigation in this field. It is obvious that cautious interpretation of these results will lead the way in the development of new alloys and their compatibility in harsh molten salt environments.

Conclusions

Three potential high-temperature alloys Nimonic 80A, Inconel 718 and Inconel C-276 were investigated for corrosion behaviour in molten FLiNaK salt at 680°C. The order of corrosion rate was Inconel C-276 < Inconel 718 < Nimonic 80A, confirmed both by weight loss measurements and electrochemical measurements. All the tested alloys suffer Cr dissolution into the molten salt, although oxide layers varied in shape and size. However, corrosion products formed on the surface remained intact, confirmed the formation of adherent oxide layers. Ni-enrichment beneath the oxide layers improves corrosion resistance by preventing the further diffusion of oxygen. Our experiments provide detailed insight of the initial stages of corrosion of the tested alloys in an accelerated corrosive environment of molten FLiNaK salts.

Acknowledgements

This work was supported by programme SASPRO (Mobility Programme of the Slovak Academy of Sciences), Marie Curie Actions of the European Union's Seventh Framework Programme under the grant agreement No. 1119/02/02. The present paper was supported by the Slovak Research and Development Agency, Project No. APVV-15-0540.

Disclosure statement

No potential conflict of interest was reported by the authors.

Funding

This work was supported by the Slovak Research and Development Agency under the contract No. APVV-15-0479 and Science Grand Agency under the contract No. Vega 2/0114/16.

Notes on contributors

Dr. Niketan S. Patel is a Marie Sklodowska Curie Fellow at Institute of Inorganic Chemistry, Bratislava, Slovakia. His main research interests are Corrosion of Metals, Electrochemistry and Molten systems.

Dr. Viliam Pavlík is a scientist at the Institute of inorganic chemistry, Bratislava, Slovakia. His research focuses on corrosion of superalloys in molten salts, especially in fluorides.

Dr. Blanka Kubíková is researcher in the department of molten systems at the Institute of Inorganic Chemistry Slovak Academy of Sciences, Bratislava. Her research is focused on physicochemical investigation of molten systems.

Dr. Martin Nosko is head of department of Microstructure of surfaces and interfaces, Institute of Materials and Machine Mechanics SAS. His research is focused on microstructural evaluation of the materials and its response to production parameters, mechanical properties and degradation mechanisms via SEM, EDS/WDS/EBSD, TEM and other characterization methods.

Dr. Vladimír Danielik is an associate professor in the Inorganic Technology department at the Slovak University of Technology, Bratislava. His research focuses on molten salts, electrochemistry, kinetics and thermodynamics.

Miroslav Boča is a senior researcher at Institute of Inorganic Chemistry Slovak Academy of Sciences, actually its director. In 2003/2004 he spent one year on Alexander von Humboldt scholarship at Darmstadt University of Technology. His research is focused on molten salts based on fluorides.

ORCID

Blanka Kubíková http://orcid.org/0000-0002-0144-1962
Vladimír Danielik http://orcid.org/0000-0002-3517-820X

References

[1] Pavlik V, Kontrik M, Boca M. Corrosion behavior of Incoloy 800H/HT in the fluoride molten salt FLiNaK+MFx (MFx=CrF3, FeF2, FeF3 and NiF2). New J Chem. 2015;39:9841–9847. DOI:10.1039/c5nj01839k.
[2] Olson LC, Ambrosek JW, Sridharan K, et al. Materials corrosion in molten LiF–NaF–KF salt. J Fluor Chem. 2009;130:67–73. DOI:10.1016/j.jfluchem.2008.05.008.
[3] Williams DF. Assessment of candidate molten salt coolants for the NGNP/NHI heat-transfer loop. National Laboratory Report ORNL/TM-2006/69; 2006. p. 1–32.
[4] Forsberg CW, Peterson PF, Zhao H. High-Temperature liquid-fluoride-salt closed-Brayton-Cycle solar power towers. J Sol Energy Eng. 2007;129:141–146. DOI:10.1115/1.2710245.
[5] Khanna AS. 2002. Introduction to high temperature oxidation and corrosion. ASM Int. ISBN 0-87170-762-4:1–322.
[6] Williams DF, Toth LM, Clarno KT. Assessment of Candidate Molten Salt Coolants for the Advanced High-Temperature Reactor (AHTR). National Laboratory Report ORNL/TM-2006/12; 2006, p. 1–69.
[7] Sohal MS, Ebner MA, Sabharwall P, et al. Engineering database of liquid salt thermophysical and thermochemical properties. National Laboratory report INL/EXT-10-18297; 2013. p. 1–59.
[8] Ouyang FY, Chang CH, You BC, et al. Effect of moisture on corrosion of Ni-based alloys in molten alkali fluoride FLiNaK salt environments. J Nucl Mater. 2013;437:201–207. DOI:10.1016/j.jnucmat.2013.02.021.
[9] Ouyang FY, Chang CH, Kai JJ. Long-term corrosion behaviors of Hastelloy-N and Hastelloy-B3 in moisture-containing molten FLiNaK salt environments. J Nucl Mater. 2014;446:81–89. DOI:10.1016/j.jnucmat.2013.11.045.
[10] Sridharan K, Anderson M, Corradini M, et al. Molten Salt Heat Transport Loop: Materials Corrosion and Heat Transfer Phenomena. Nuclear Energy Research Initiative (NERI) Final Report, University of Wisconsin, WI; 2008.
[11] Sridharan K. Liquid Salts as Media for Process Heat Transfer from VHTRs: Forced Convective Channel Flow Thermal Hydraulics, Materials, and Coatings. Nuclear Energy Research Initiative (NERI) Project Review, NERI 07-030, University of Wisconsin, WI; 2009.
[12] Patel NS, Pavlík V, Boča M. High-Temperature corrosion behavior of superalloys in molten salts – A review. Crit. Rev. Solid State Mater. Sci. 2017;42:83–97. DOI:10.1080/10408436.2016.1243090.
[13] Turkdogan ET. Physical chemistry of high temperature technology. New York: Academic Press; 1980; p. 524.
[14] Lim JH, Jung WJ. Corrosion behavior of superalloys in a LiCl-Li_2O molten salt. Mater Trans. 2014;55:1618–1622. DOI:10.2320/matertrans.M2013262.
[15] Cho SH, Oh SC, Park SB, et al. High temperature corrosion behavior of Ni-based alloys. Met Mater Int. 2012;18:939–949. DOI:10.1007/s12540-012-6005-4.
[16] Cho SH, Hur JM, Seo CS, et al. High temperature corrosion of superalloys in a molten salt under an oxidizing atmosphere. J Alloys Compd. 2008;452:11–15. DOI:10.1016/j.jallcom.2007.01.169.
[17] Lai GY. Molten salt corrosion (chapter 15). In: Lai GY, editor. High-Temperature corrosion and materials applications. OH: ASM International; 2007. p. 409–421. ISBN 0-87170-853-1.
[18] Vignarooban K, Pugazhendhi P, Tucker C, et al. Corrosion resistance of Hastelloys in molten metal-chloride heat-transfer fluids for concentrating solar power applications. Sol Energy. 2014;103:62–69. DOI:10.1016/j.solener.2014.02.002.
[19] Wang Y, Liu H, Zeng C. Galvanic corrosion of pure metals in molten fluorides. J Fluor Chem. 2014;165:1–6. DOI:10.1016/j.jfluchem.2014.05.010.